Electronic Supplementary Material (ESI) for Journal of Materials Chemistry C.

Supporting Information

Modulation of π-linker in asymmetric thermally activated delayed fluorescence molecules enabling high performance OLEDs

Weichun Wei, Zhan Yang, Xiaojie Chen, Tiantian Liu, Zhu Mao,* Juan Zhao,* and Zhenguo Chi*

1. Experimental Section

1.1 General Methods

Hydrogen (^{1}H) and carbon (^{13}C) nuclear magnetic resonance (NMR) spectra were measured using a Bruker AvanceIII 500HD spectrometer, with deuterated dimethylsulfoxide (DMSO-d_6) and chloroform ($CDCl_3$) as solvent and tetramethylsilane (TMS) as an internal reference. High resolution mass spectra (HRMS) was collected from Thermo MAT95XP spectrometer, respectively. Elemental analysis was conducted using an Elementar Vario EL analyzer. Photoluminescence (PL) spectra and UV-vis absorption spectra were measured using a Shimadzu RF-5301PC spectrometer and a Hitachi U-3900 spectrophotometer, respectively. Transient PL decay characteristics were recorded on a Horiba FL-3 system equipped with Oxford Optistat DN. PL quantum yields were recorded on a Horiba JY FL-3 spectrometer equipped with a calibrated integrating sphere. Cyclic voltammetry measurements were carried out on a electrochemical workstation VMP300 (Bio-Logic), by using tetrabutylammoniumhexafluorophosphate ($TBAPF_6$, 0.1 M) in dichloromethane as electrolyte, a platinum as counter electrode, and a Ag/AgCl as reference electrode (versus ferrocene F_c/F_c^+). Differential scanning calorimetry (DSC) was performed using a NETZSCH DSC 204 F1 thermal analyzer at a heating rate of 10 ℃ min^{-1} under a N_2 atmosphere. Thermogravimetric analyses (TGA) were performed with a TA thermal analyzer (A50) under a N_2 atmosphere with a heating rate of 20 ℃ min^{-1}. Timedependent Density Functional Theory (TD-DFT) calculations were performed with Gaussian 09W program package and produced by B3LYP/6-311G*.[1] Spin-orbit coupling (SOC) matrix were obtained though PySOC program based on the TD-DFT results.[2] Natural transition orbital (NTO) calculations were carried out by Multiwfn program.[3] Single-crystal X-ray data were determined using an Oxford Diffraction Germini S Ultra X-ray Single Crystal Diffractometer with a (Cu) X-ray source. Single crystals were obtained through slow evaporation of saturated solution consisting of ethanol and dichloromethane mixed solvents (CCDC number of SCP, PCz, 2PCz, PSz and 2PSz are 981368, 1421266, 1966103, 1966101, 1966102. These data can be obtained free of charge from The Cambridge Crystallographic Data Centre via www.ccdc.cam.ac.uk/data_request/cif.)

1.2 Devices Fabrication and Characterization

Indium tin oxide (ITO) coated glass substrates with a sheet resistance of 8 Ω sq^{-1} were firstly ultrasonically cleaned. Then, PEDOT:PSS was spin-coated on the cleaned ITO at a speed of 2000 rpm for 60 seconds, following by thermal annealing treatment for 15 minutes at 200 °C in air. Subsequently, the PEDOT:PSS coated ITO substrates were transferred to a thermal evaporation chamber for deposition of organic and metals layers under vacuum pressure of 4×10^{-4} Pa. The finished devices had an active area of 9 mm^2. The current density−voltage−luminance characteristics and electroluminescent (EL) spectra of the unsealed OLEDs were measured using a Keithley 2400 source combined with a Photo Research PR735 spectrometer at room temperature, while the external quantum efficiencies (EQEs) were calculated using a computer program based on previously reported theory.

1.3 Materials

Poly(3,4-ethylenedioxythiophene):poly(styrenesulfonate) (PEDOT:PSS), m-bis(N-carbazolyl)benzene (MCP) and 1,3,5-tris(N-phenylbenzimidazol-2-yl)benzene (TPBI) were used as purchased from Xi'an Polymer Light Technology Co. Ltd. All the chemicals were used as received without any purification.

2. Synthesis and characterization

SCP and PCz were synthesized according to our previous report,[4,5] and 2PCz, PSz and 2PSz were synthesized as below in Scheme S1-S3.

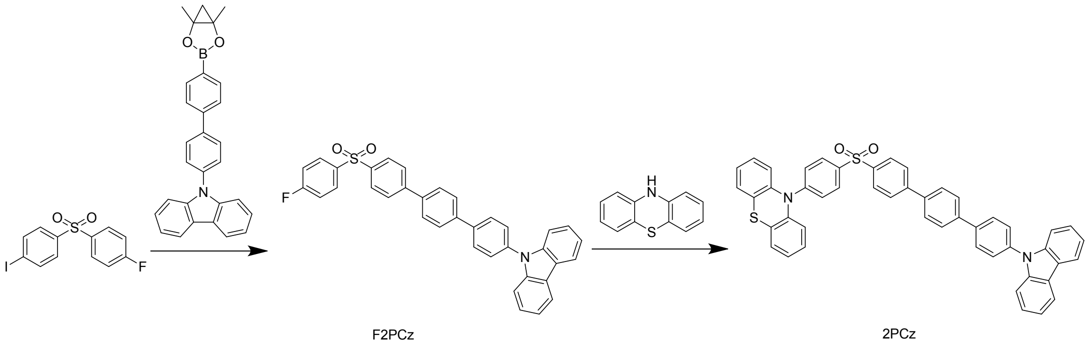

Scheme S1. Synthetic routes for 2PCz.

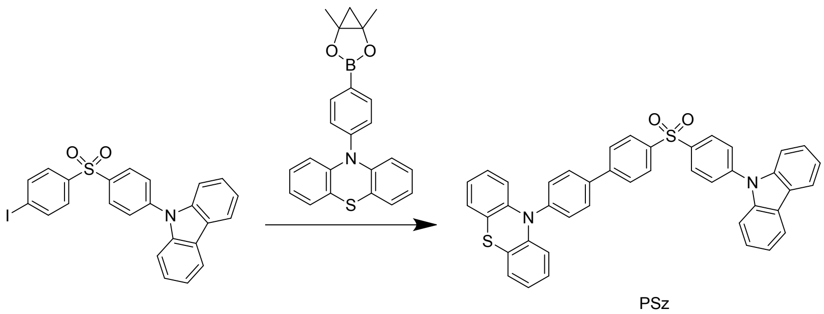

Scheme S2. Synthetic routes for PSz.

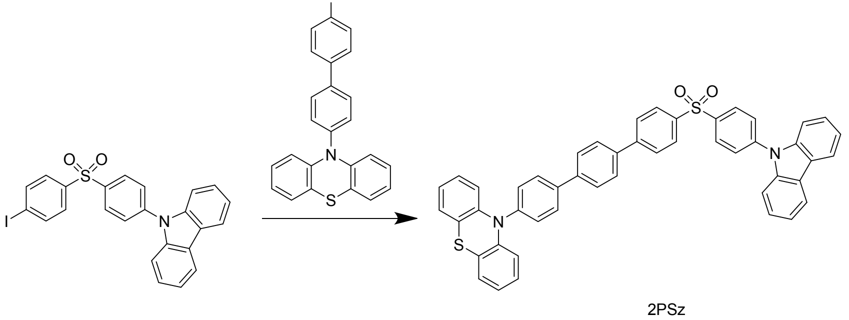

Scheme S3. Synthetic routes for 2PSz.

Synthesis of 9-(4''-((4-fluorophenyl)sulfonyl)-[1,1':4',1''-terphenyl]-4-yl)-9H-carbazole (F2PCz)

9-(4''-((4-fluorophenyl)sulfonyl)-[1,1':4',1''-terphenyl]-4-yl)-9H-carbazole (2.00 g, 4.66 mmol) and 1-fluoro-4-((4-iodophenyl)sulfonyl)benzene (1.54 g, 4.24 mmol) were dissolved in THF (30 mL), then 8 M K_2CO_3 solution (4 mL) was added. Then catalytic amount of $Pd(PPh_3)_4$ was added into the mixture under an argon atmosphere. The resulting mixture was stirred at 80 ˚C for 12 h. After cooling down to ambient temperature, the product was purified by silica gel column chromatography with dichloromethane/n-hexane (v/v=1:2) as eluent. Compound F2PCz was obtained as a white powder in 33% yield (0.8 g).

Synthesis of 10-(4-((4''-(9H-carbazol-9-yl)-[1,1':4',1''-terphenyl]-4-yl)sulfonyl)phenyl)-10H-phenothiazine (2PCz)

Phenothiazine (0.32 g, 1.62 mmol), compound FSPh2Cz (0.6 g, 1.08 mmol), potassium tert-butoxide (t-BuOK) (0.21 g, 2.17 mmol) were dissolved in DMF (10 ml) at 0 ℃. The resulting mixture was stirred at 100 ℃ for 12 h, then cooled to room temperature. The mixture was poured to 100 ml of salt water, the crude product was collected by filtration. The product was purified by silica gel column chromatography with dichloromethane/n-hexane (v/v=3:1) as eluent. Compound 2PCz was obtained as a yellow powder in 50% yield (0.4 g).

Synthesis of 10-(4'-((4-(9H-carbazol-9-yl)phenyl)sulfonyl)-[1,1'-biphenyl]-4-yl)-10H-phenothiazine (PSz)

9-(4-((4-iodophenyl)sulfonyl)phenyl)-9H-carbazole (1.00 g, 1.02 mmol) and 10-(4-(1,5-dimethyl-2,4-dioxa-3-borabicyclo[3.1.0]hexan-3-yl)phenyl)-10H-phenothiazine (0.85 g, 2.01mmol) were dissolved in THF (15 mL), then 4 M K_2CO_3 solution (2 mL) was added. Then catalytic amount of $Pd(PPh_3)_4$ was added into the mixture under an argon atmosphere. The resulting mixture was stirred at 80 ˚C for 12 h. After cooling down to ambient temperature, the product was purified by silica gel column chromatography with dichloromethane/n-hexane (v/v=1:1) as eluent. Compound PSz was obtained as a yellow powder in 45% yield (0.6 g).

Synthesis of 10-(4''-((4-(9H-carbazol-9-yl)phenyl)sulfonyl)-[1,1':4',1''-terphenyl]-4-yl)-10H-phenothiazine (2PSz)

9-(4-((4-iodophenyl)sulfonyl)phenyl)-9H-carbazole (1.32 g, 2.60 mmol) and 10-(4'-(1,5-dimethyl-2,4-dioxa-3-borabicyclo[3.1.0]hexan-3-yl)-[1,1'-biphenyl]-4-yl)-10H-phenothiazine (0.80 g, 1.73 mmol) were dissolved in THF (20 mL), then 4 M K_2CO_3 solution (2 mL) was added. Then catalytic amount of $Pd(PPh_3)_4$ was added into the mixture under an argon atmosphere. The resulting mixture was stirred at 80 ˚C for 12 h. After cooling down to ambient temperature, the product was purified by silica gel column chromatography with dichloromethane/n-hexane (v/v=1:1) as eluent. Compound 2PSz was obtained as a yellow powder in 30% yield (0.3 g).

2. Supplementary Figures and Tables

^{1}H NMR (400 MHz, DMSO) δ = 8.28 (d, *J* = 7.7 Hz, 2H), 8.17 – 7.87 (m, 12H), 7.76 (d, *J* = 8.5 Hz, 2H), 7.58 – 7.40 (m, 6H), 7.32 (ddd, *J* = 8.0, 5.6, 2.5 Hz, 2H).

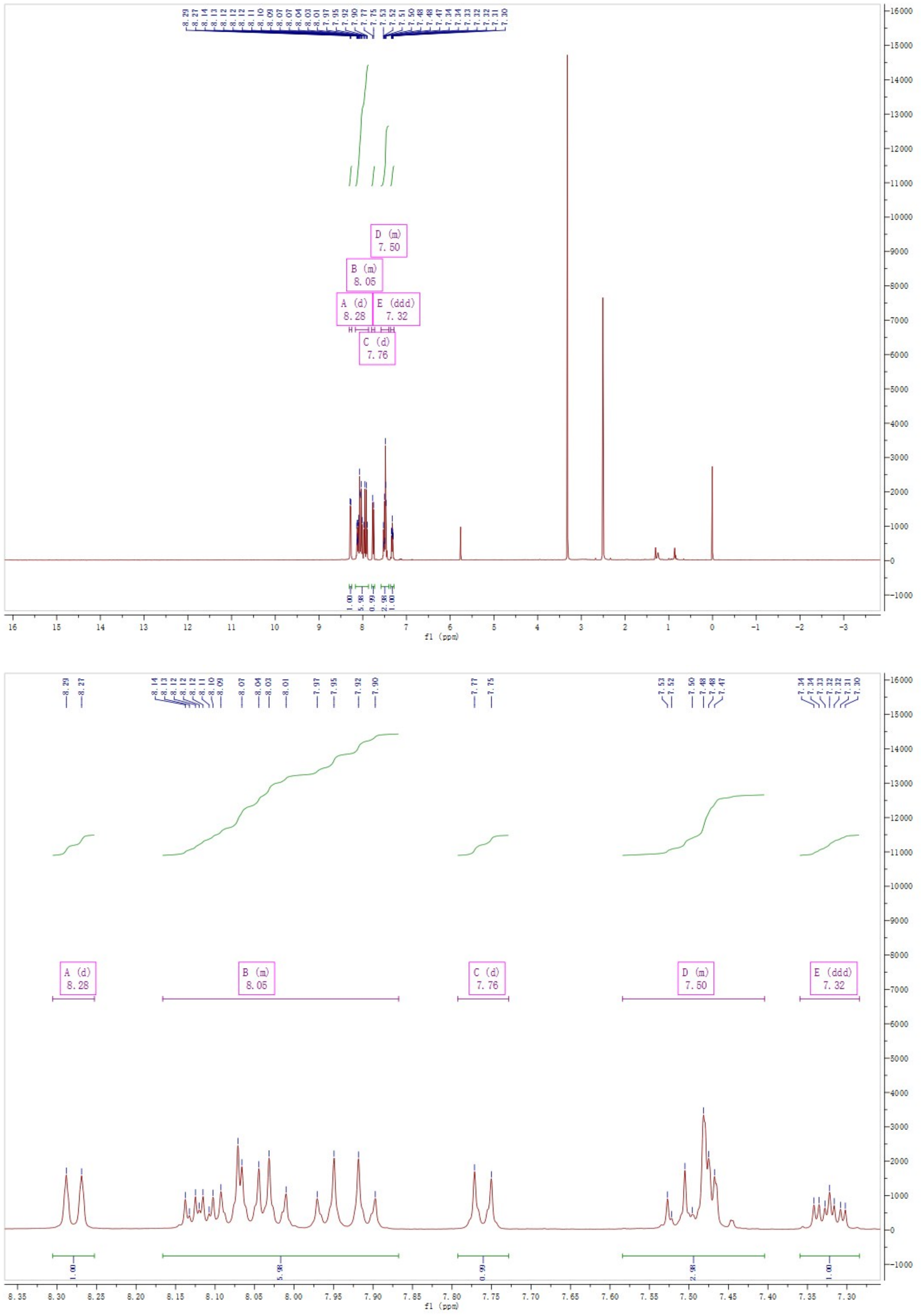

Figure S1. ^{1}H NMR spectra of F2PCz.

^{1}H NMR (400 MHz, DMSO) δ= 8.28 (d, *J* = 7.8 Hz, 2H), 8.12 – 7.85 (m, 12H), 7.76 (d, *J* = 8.5 Hz, 2H), 7.55 (d, *J* = 7.4 Hz, 2H), 7.48 (s, 4H), 7.40 (s, 4H), 7.31 (tdt, *J* = 8.6, 5.6, 4.4 Hz, 4H), 7.13 (t, *J* = 8.2 Hz, 2H).

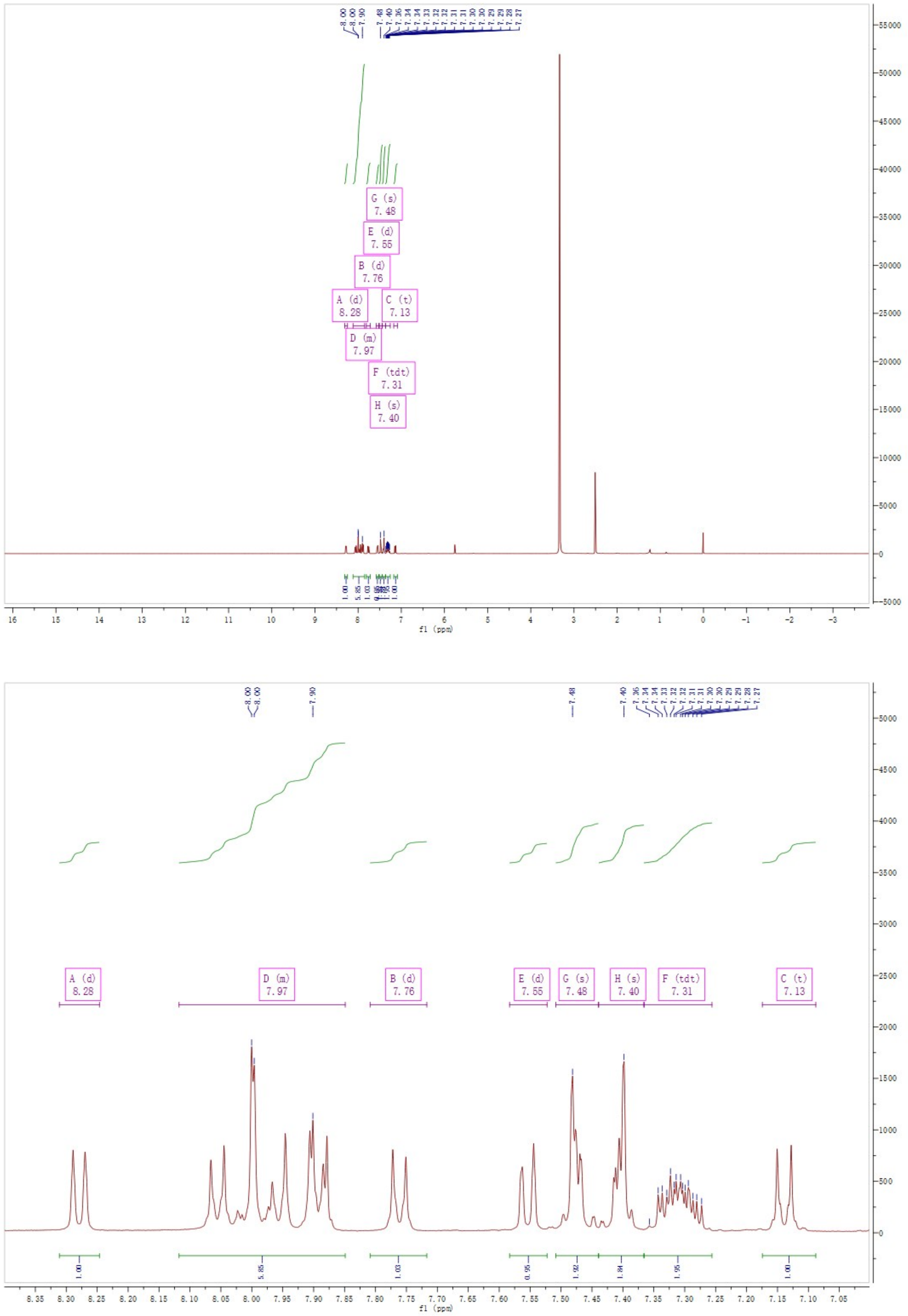

Figure S2. ^{1}H NMR spectra of 2PCz.

^{13}C NMR (126 MHz, $CDCl_3$) δ=149.49, 145.12, 141.28 – 140.76, 140.76 – 140.60, 140.39, 139.27, 138.47, 137.27, 133.37, 133.13, 129.45, 128.86, 128.43, 127.84, 127.40, 126.27, 126.26 – 125.70, 123.48, 120.37, 120.07, 116.45, 109.81.

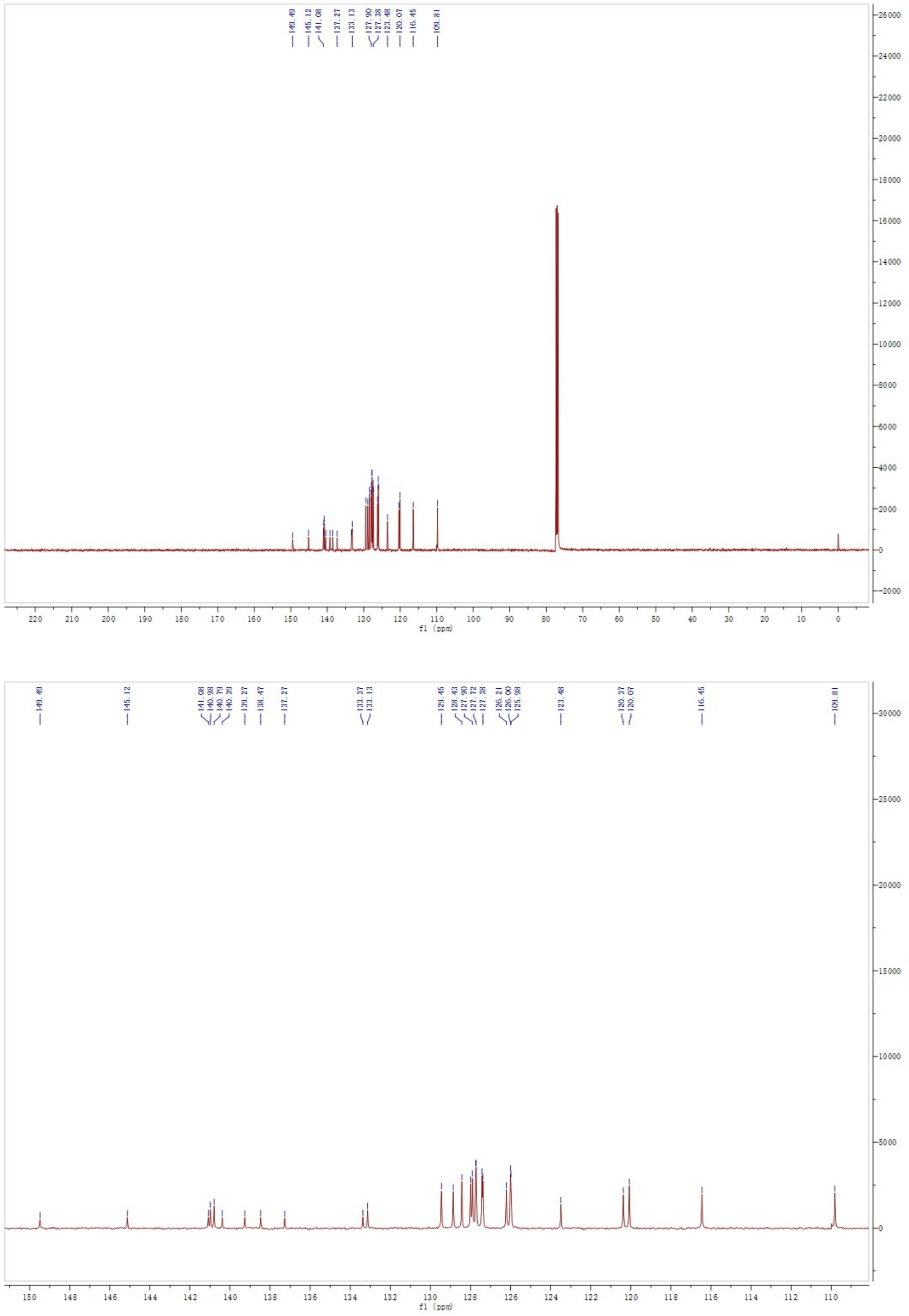

Figure S3. ^{13}C NMR spectra of 2PCz.

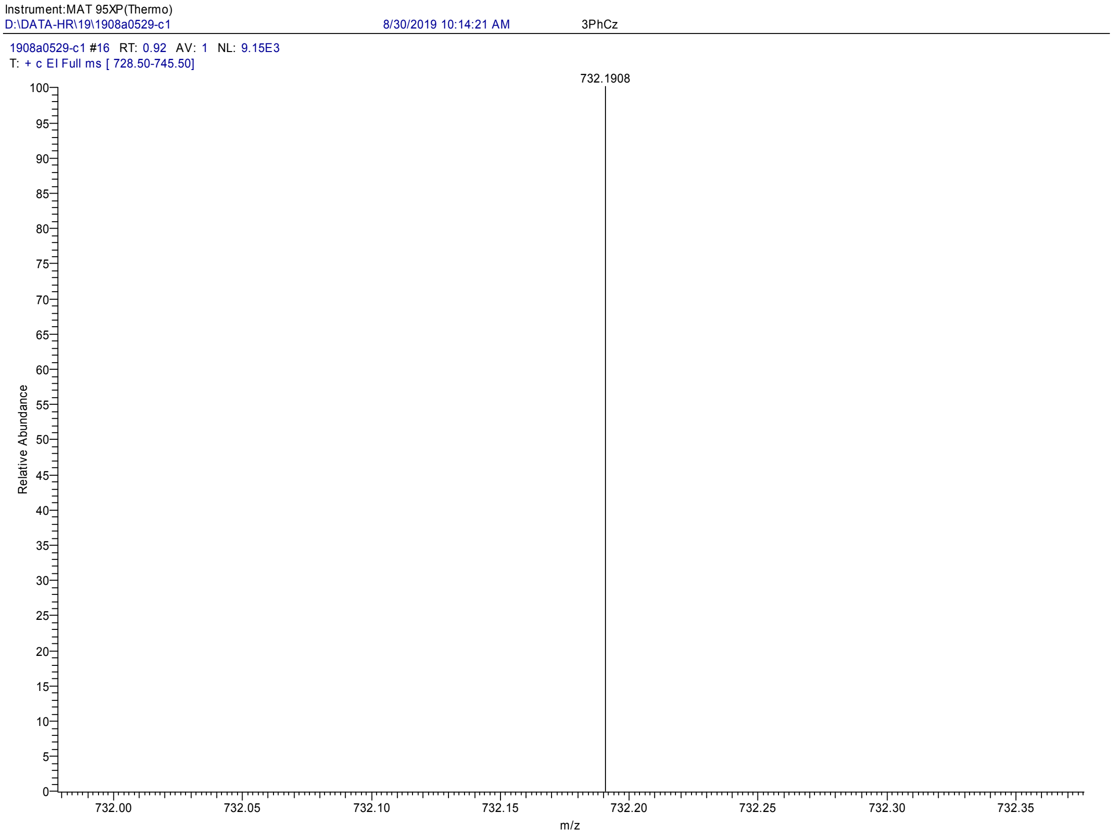

Figure S4. High resolution mass spectrum of 2PCz.

^{1}H NMR (500 MHz, DMSO) δ = 8.26 (dd, *J* = 18.4, 8.2 Hz, 9H), 8.16 (d, *J* = 8.6 Hz, 5H), 8.03 (d, *J* = 8.6 Hz, 5H), 7.95 (t, *J* = 8.1 Hz, 9H), 7.53 – 7.38 (m, 14H), 7.31 (t, *J* = 7.2 Hz, 5H), 7.15 (dd, *J* = 7.6, 1.4 Hz, 5H), 7.00 (dd, *J* = 7.8, 1.1 Hz, 4H), 6.92 (td, *J* = 7.5, 1.1 Hz, 5H), 6.41 (dd, *J* = 8.2, 0.8 Hz, 4H), 3.31 (s, 29H), 2.53 – 2.44 (m, 18H), -0.02 (s, 1H).

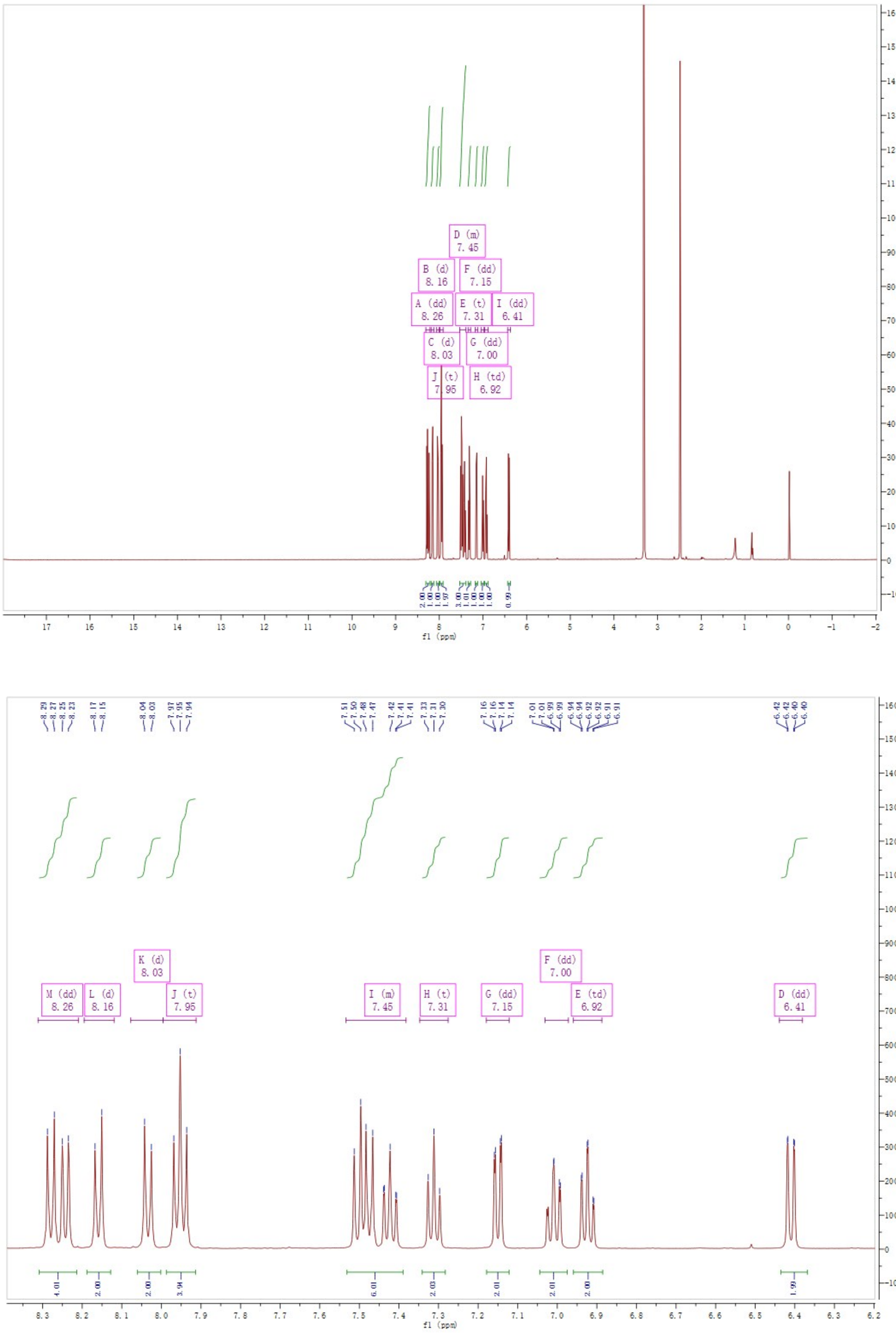

Figure S5. ^{1}H NMR spectra of PSz.

^{13}C NMR (126 MHz, $CDCl_3$) δ = 145.42, 142.55, 140.07, 139.99, 139.88, 137.82, 129.54, 128.53, 128.05, 127.19, 127.04, 126.35, 123.99, 123.38, 120.97, 120.57, 117.66, 109.61.

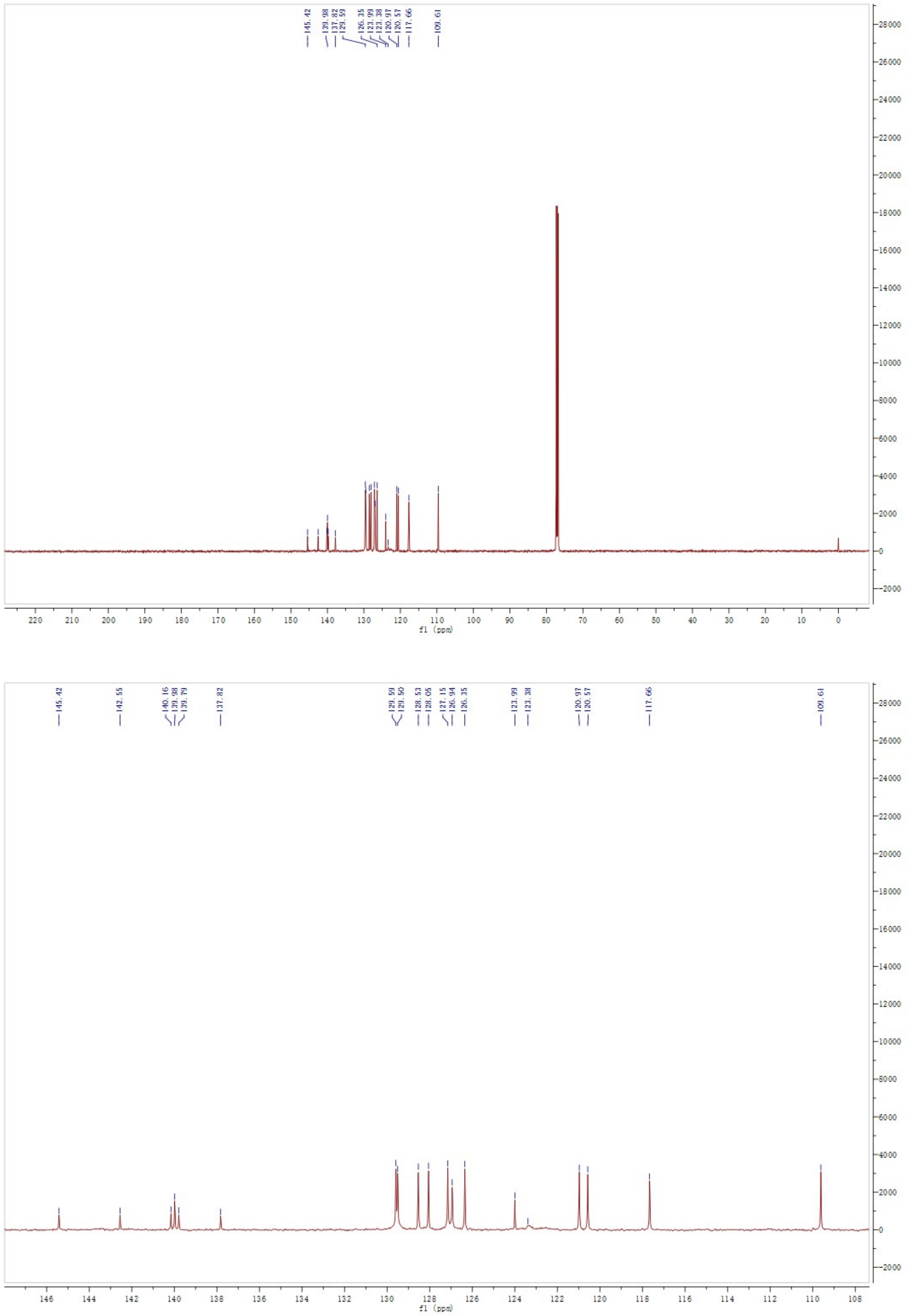

Figure S6. ^{13}C NMR spectra of PSz.

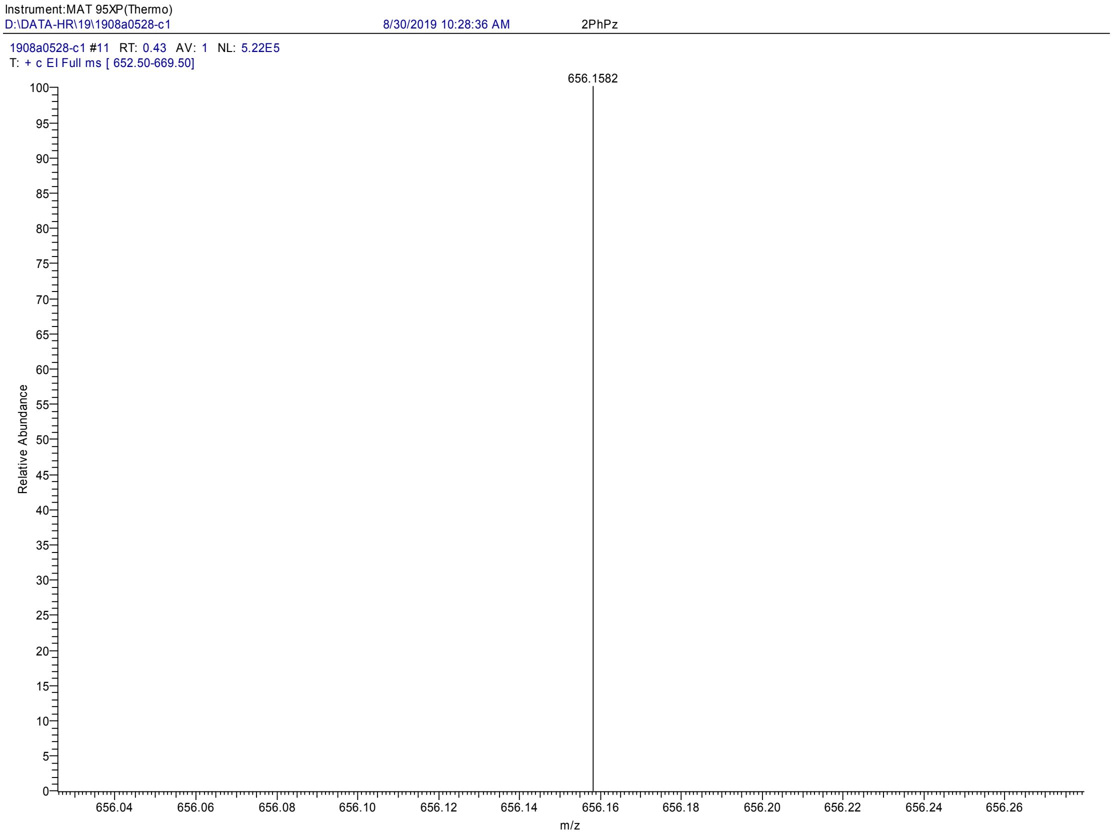

Figure S7. High resolution mass spectrum of PSz.

^{1}H NMR (500 MHz, DMSO) δ = 8.26 (dd, *J* = 18.4, 8.2 Hz, 4H), 8.16 (d, *J* = 8.6 Hz, 2H), 8.03 (d, *J* = 8.6 Hz, 2H), 7.95 (t, *J* = 8.1 Hz, 4H), 7.54 – 7.38 (m, 6H), 7.31 (t, *J* = 7.2 Hz, 2H), 7.15 (dd, *J* = 7.6, 1.4 Hz, 2H), 7.00 (dd, *J* = 7.8, 1.1 Hz, 2H), 6.92 (td, *J* = 7.5, 1.1 Hz, 2H), 6.41 (dd, *J* = 8.2, 0.8 Hz, 2H).

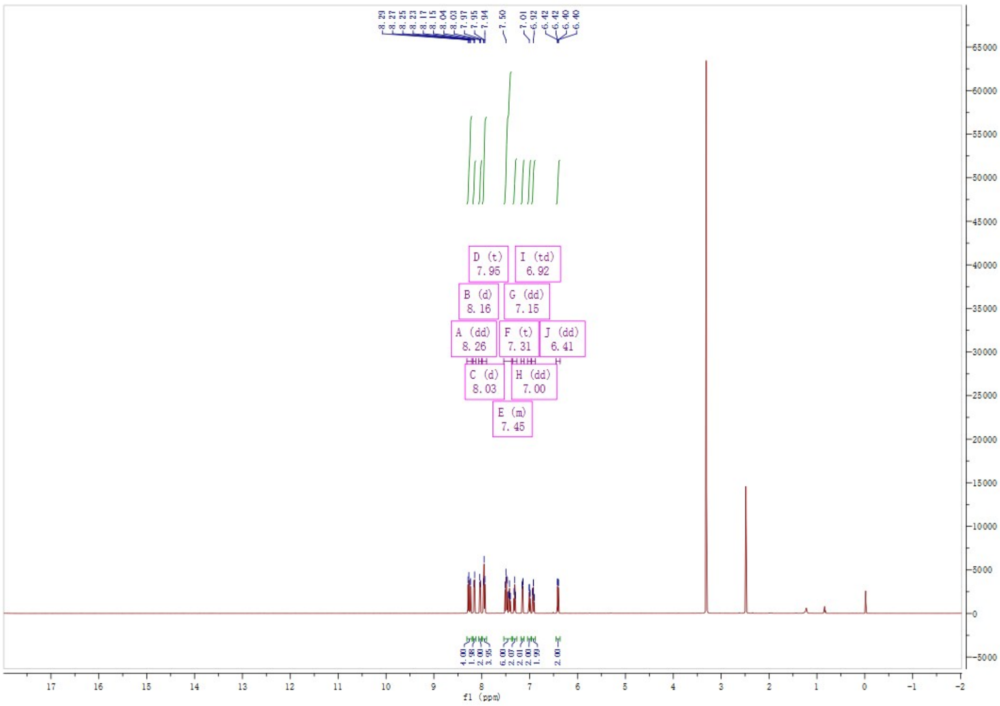

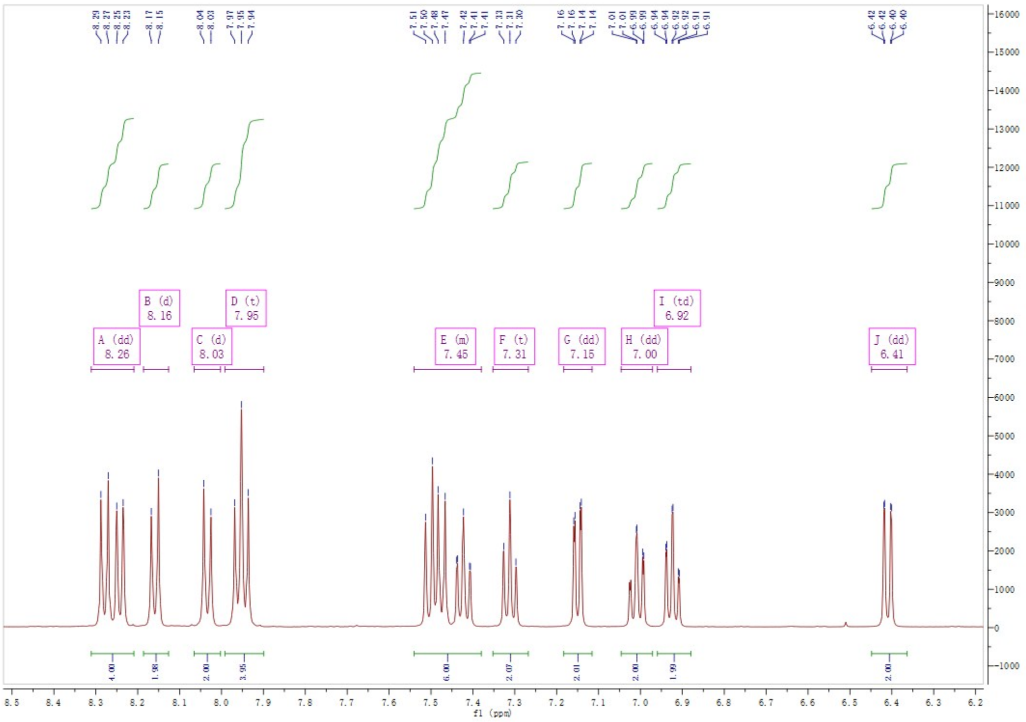

Figure S8. ^{1}H NMR spectra of 2PSz.

^{13}C NMR (126 MHz, CDCl$_3$) δ = 145.79, 142.52, 140.50, 139.92, 139.65, 138.28, 129.58, 129.27, 128.50, 128.27 – 127.62, 127.35 – 127.25, 127.01, 126.34, 123.99, 120.95, 120.56, 116.67, 109.62.

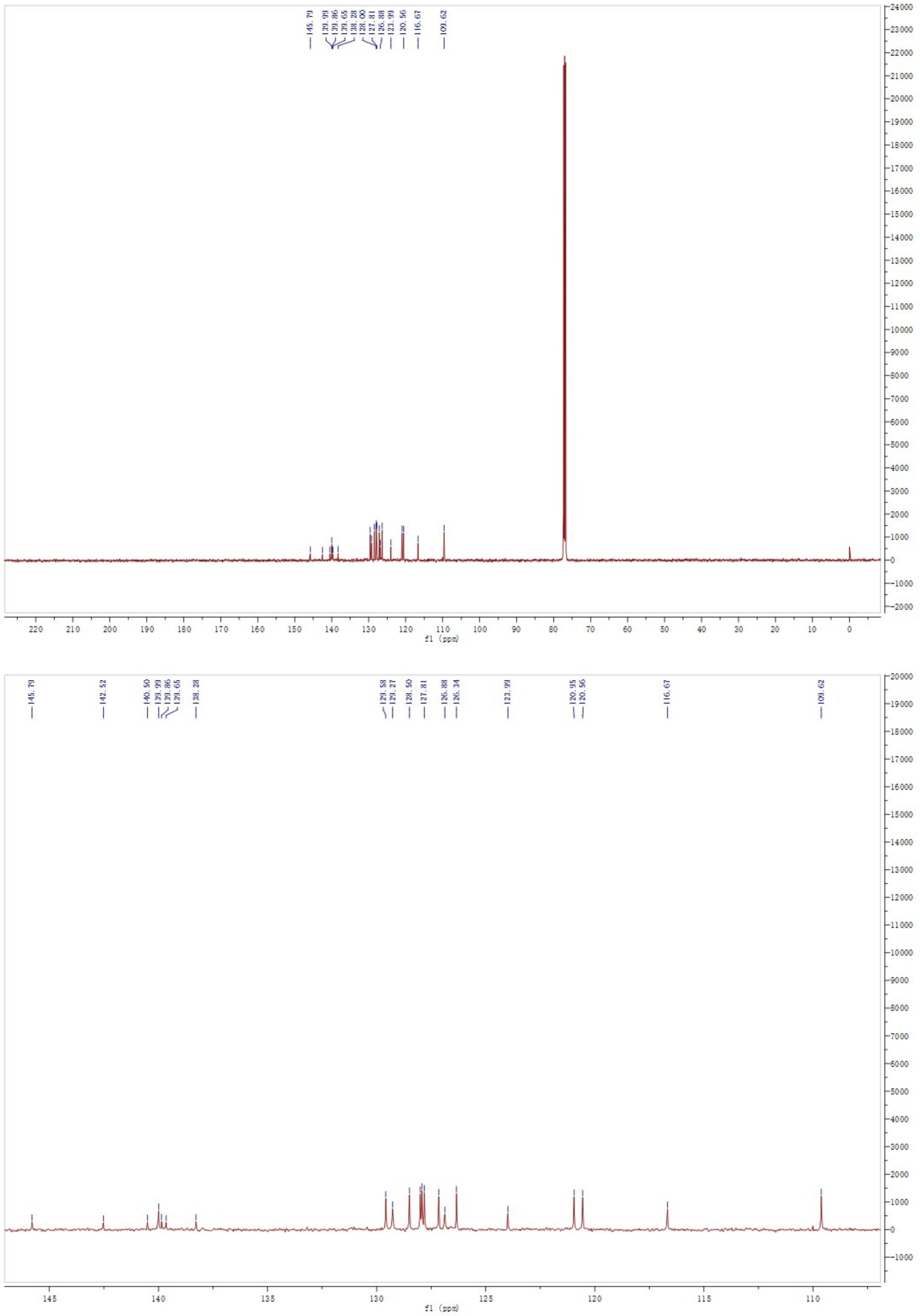

Figure S9. ^{13}C NMR spectra of 2PSz.

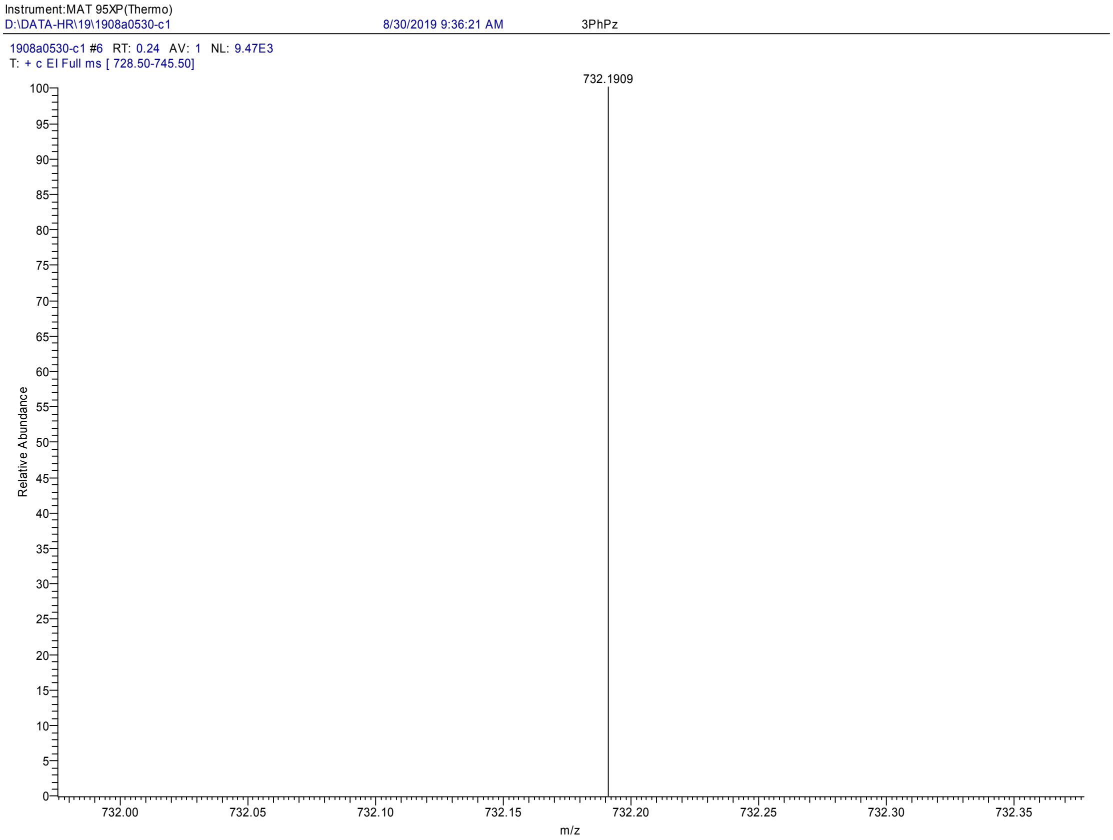

Figure S10. High resolution mass spectrum of 2PSz.

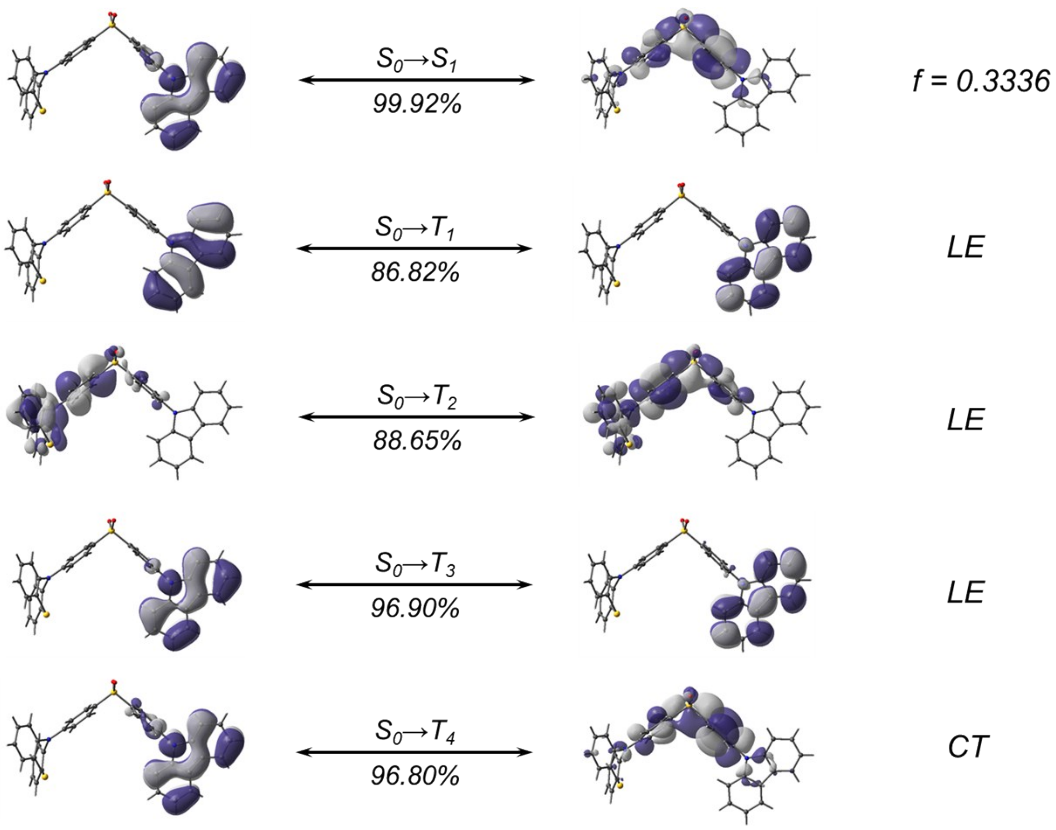

Figure S11. NTO analysis of SCP.

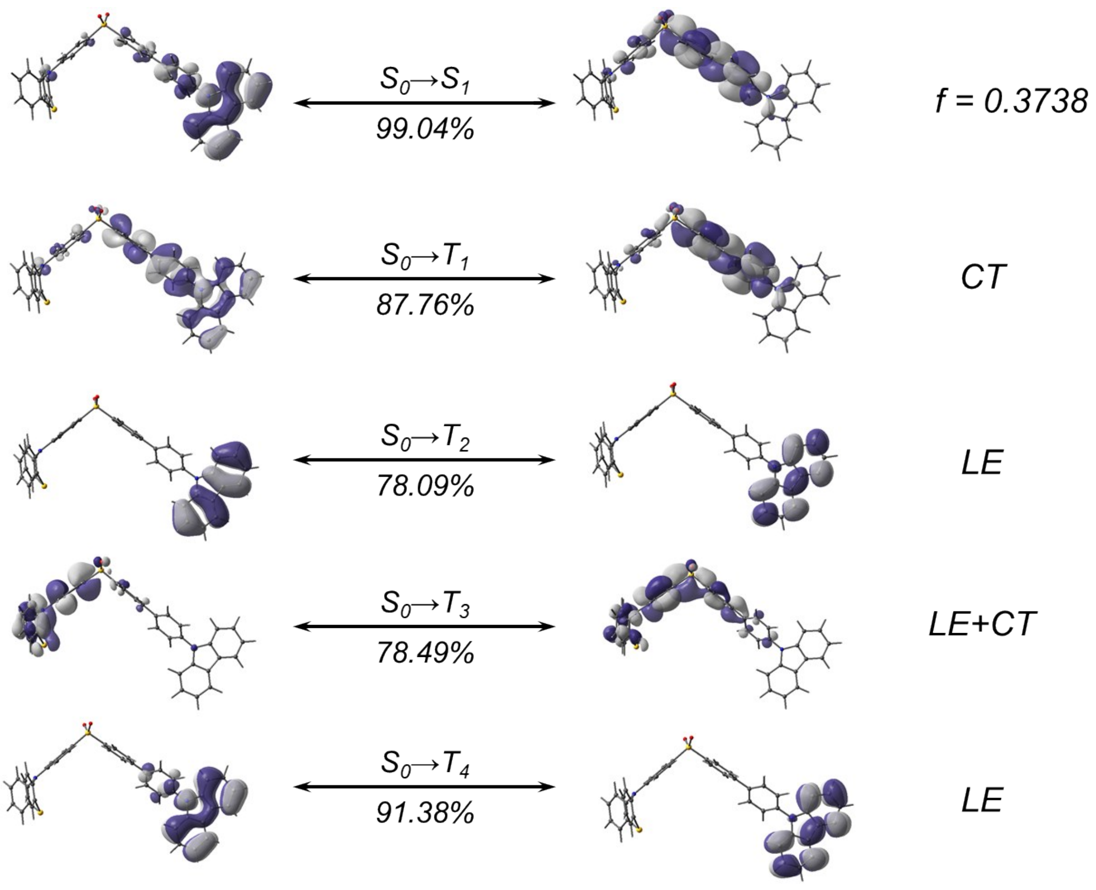

Figure S12. NTO analysis of PCz.

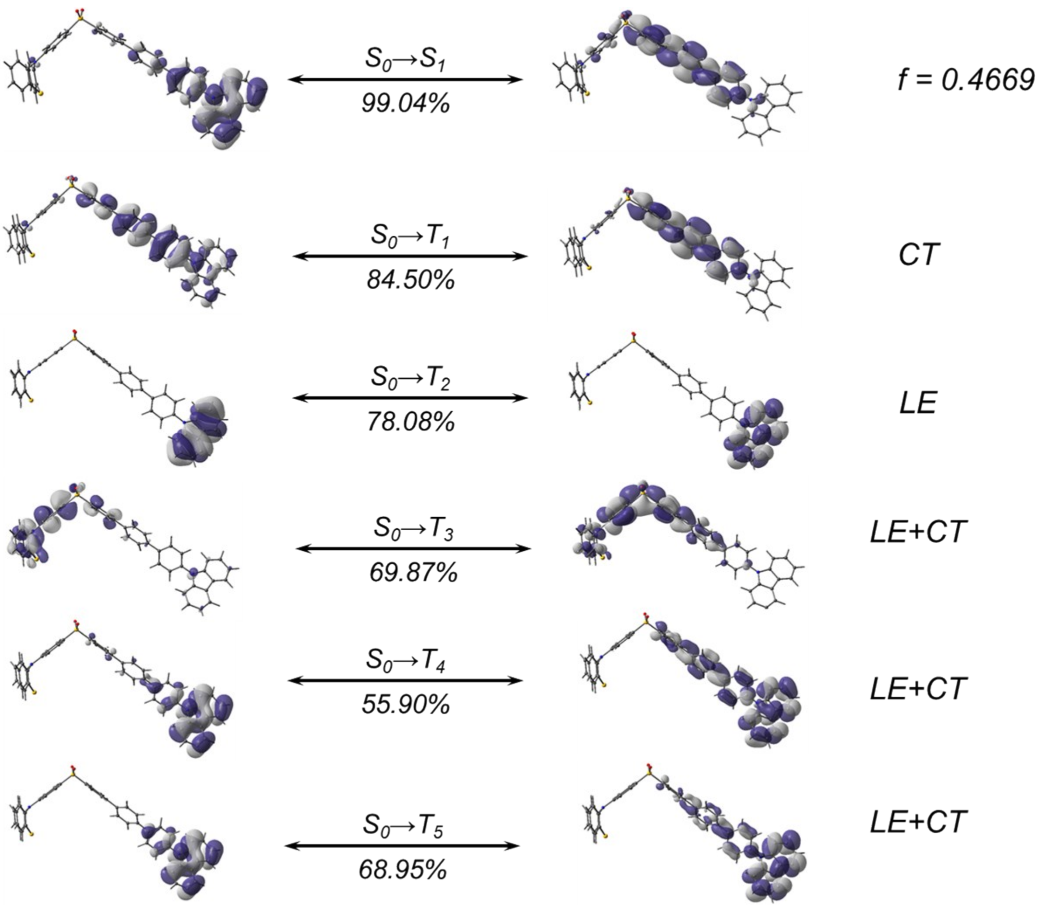

Figure S13. NTO analysis of 2PCz.

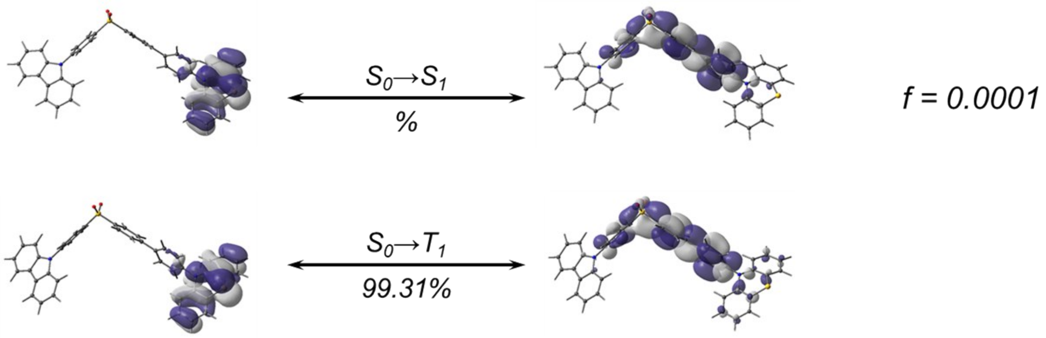

Figure S14. NTO analysis-PSz.

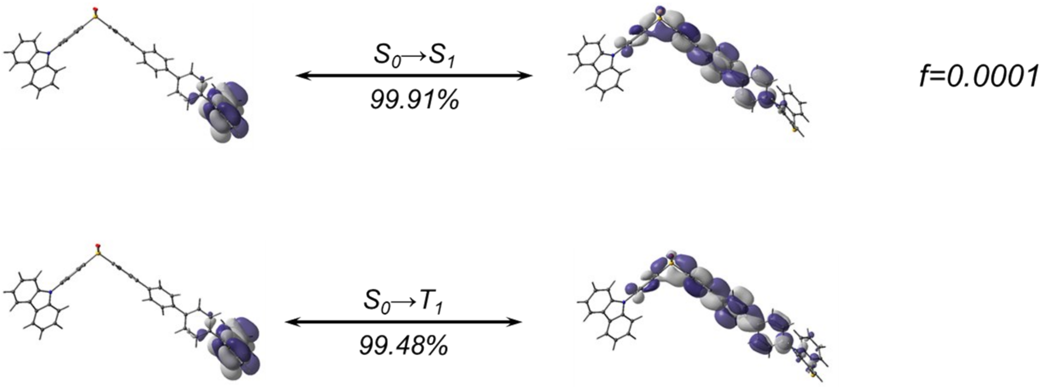

Figure S15. NTO analysis of 2PSz.

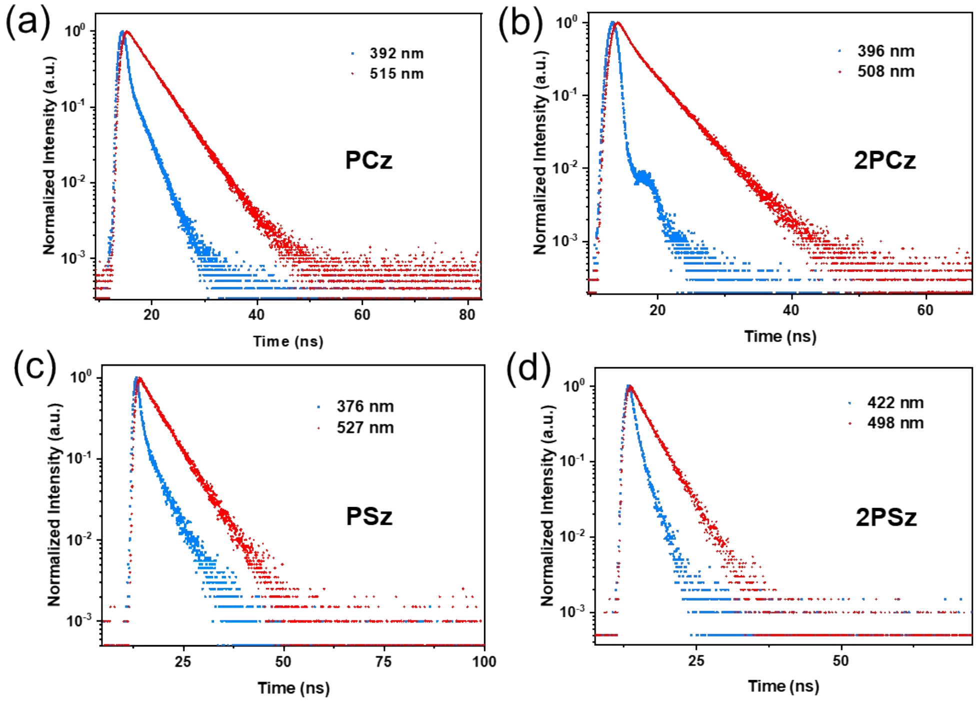

Figure S16. Lifetime curves of emission peaks in (a) **PCz**, (b) **2PCz**, (c) **PSz** and (d) **2PSz**.

Table S1 Lifetime data of emission peaks for the compounds.

Compound	λ_1 (nm)	τ_1 (ns)	λ_2 (nm)	τ_2 (ns)
PCz	392	2.45	515	4.24
2PCz	396	0.51	508	4.10
PSz	376	3.72	527	5.28
2PSz	422	1.46	498	3.21

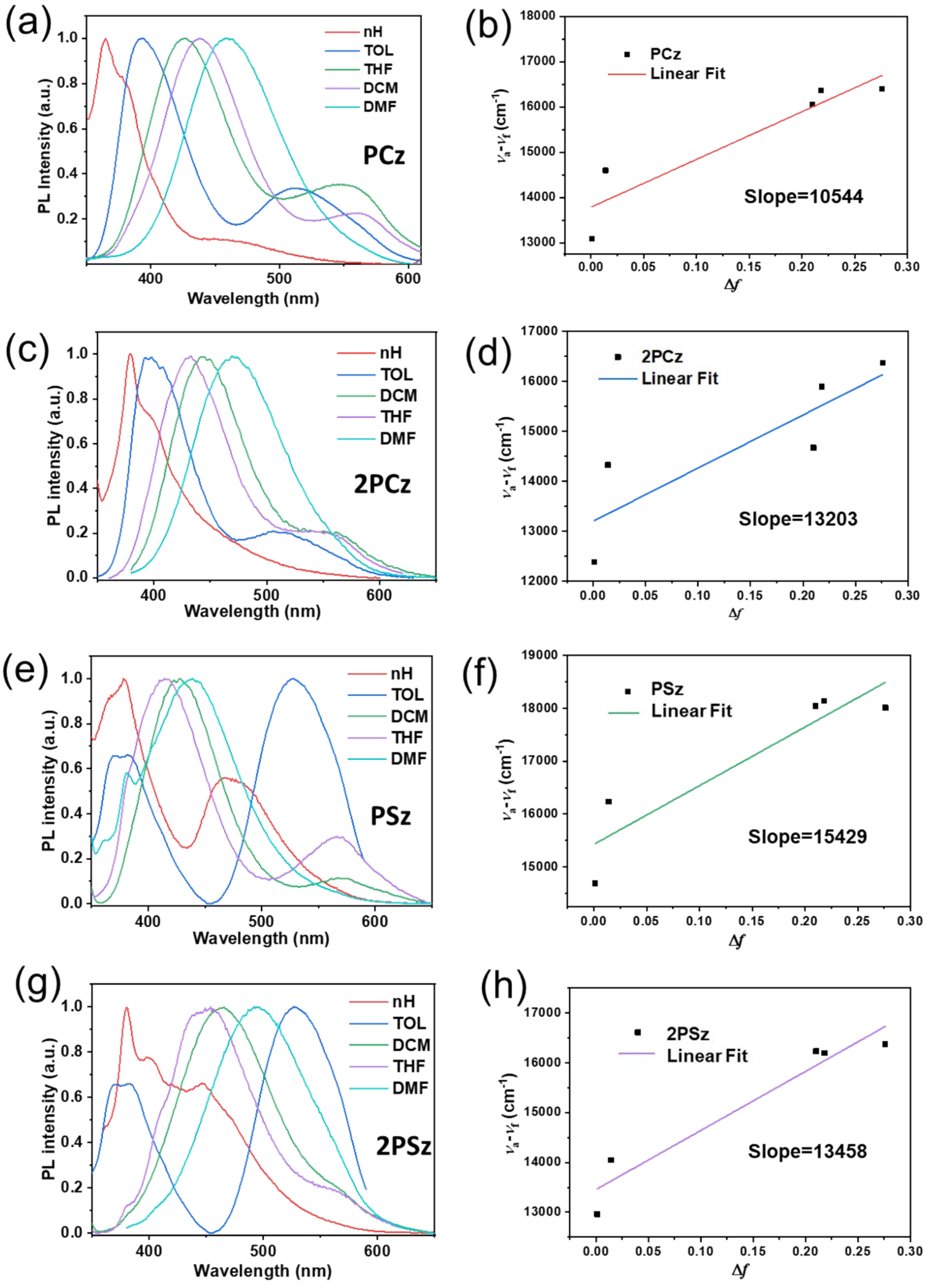

Figure S17. (a, c, e, g) PL spectral peaks of **PCz**, **2PCz**, **PSz** and **2PSz** in solutions with different solvent polarities, and (b, d, f, h) Stokes shift (v_a–v_f) as a function of orientation polarization (*f*) of solvents according to the Lippert–Mataga equation.

Table S2 PL spectral peaks in solutions with different solvent polarities.

Solvent	nH (nm)	TOL (nm)	DCM (nm)	THF (nm)	DMF (nm)
PCz	365, 470	392, 515	438, 563	426, 553	460, 563
2PCz	379, 394	396, 508	444, 552	432, 514	470, 563
PSz	371, 467	376, 527	427, 569	414, 566	439, 569
2PSz	399, 447	422, 498	464, 555	449, 554	494, 563

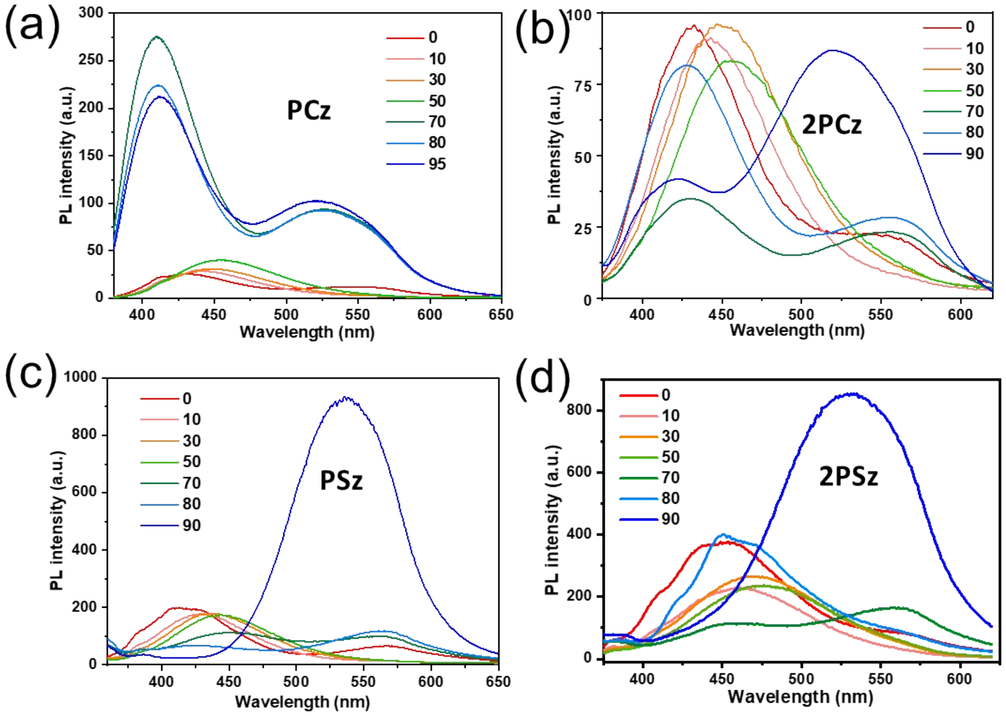

Figure S18. PL intensity of (a) **PCz**, (b) **2PCz**, (c) **PSz** and (d) **2PSz** as a function of water ratio (%) in H_2O/THF mixed solutions.

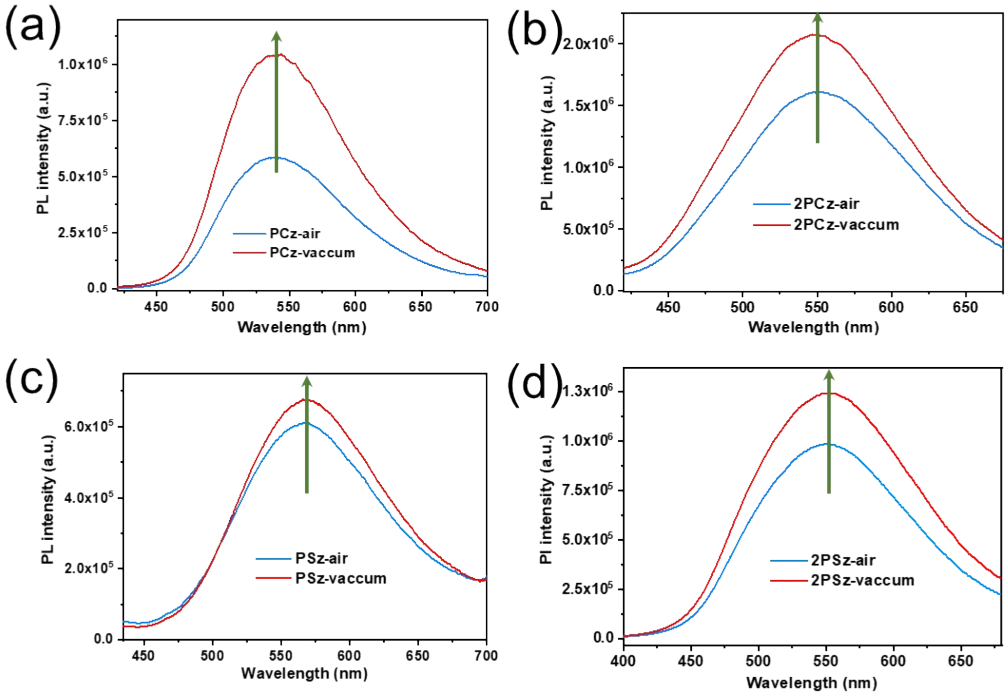

Figure S19. PL spectra of (a) **PCz**, (b) **2PCz**, (c) **PSz** and (d) **2PSz** films in air and in vacuum.

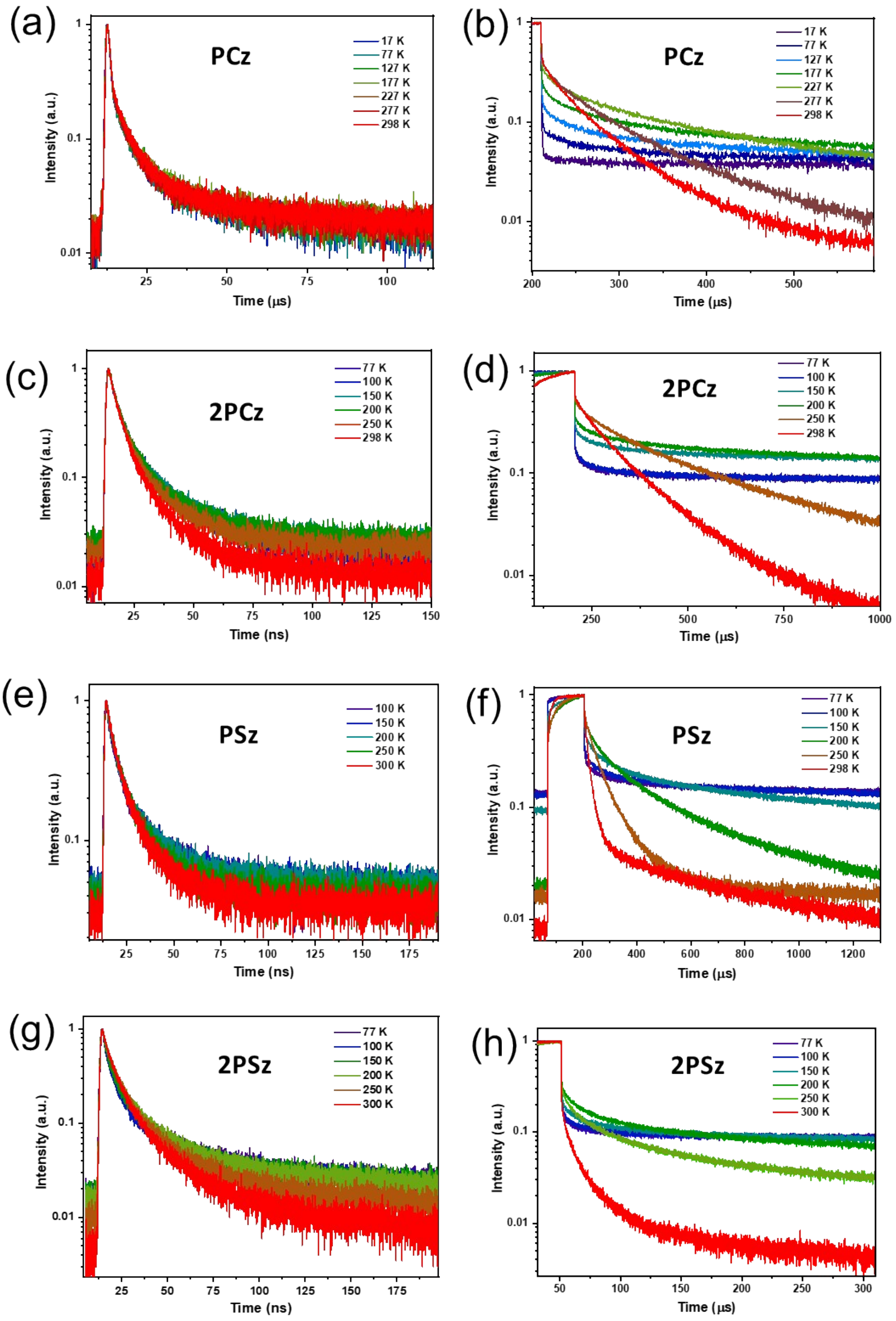

Figure S20. (a, c, e, g) prompt lifetime, and (b, d, f, h) decayed lifetime curves of **PCz**, **2PCz**, **PSz** and **2PSz** .

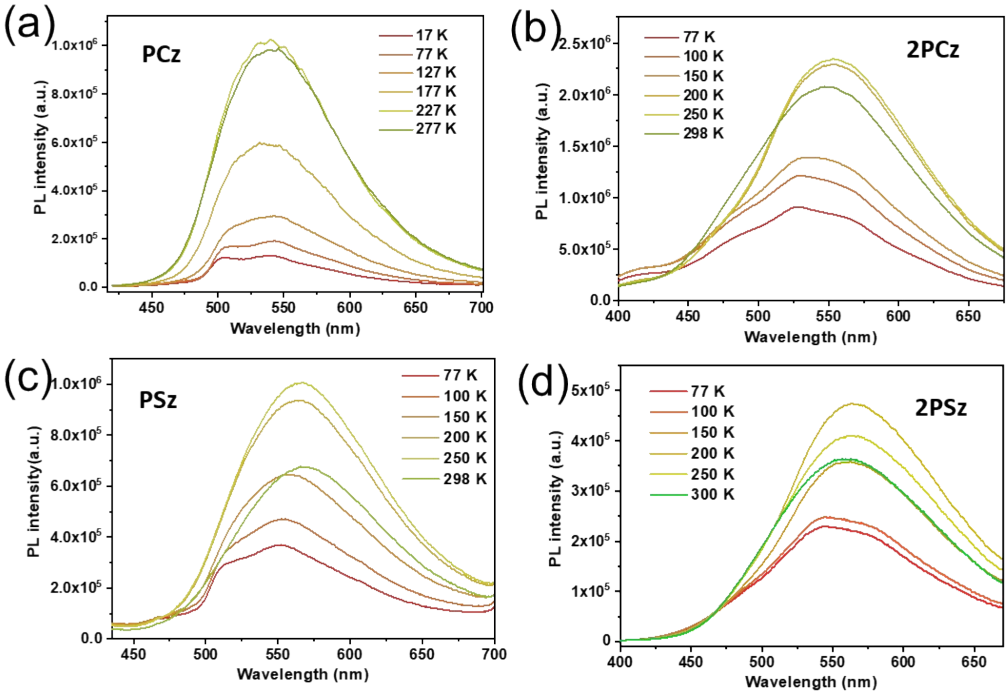

Figure S21. Temperature dependent steady-state spectra of (a) **PCz**, (b) **2PCz**, (c) **PSz** and (d) **2PSz** films carried out at different temperatures.

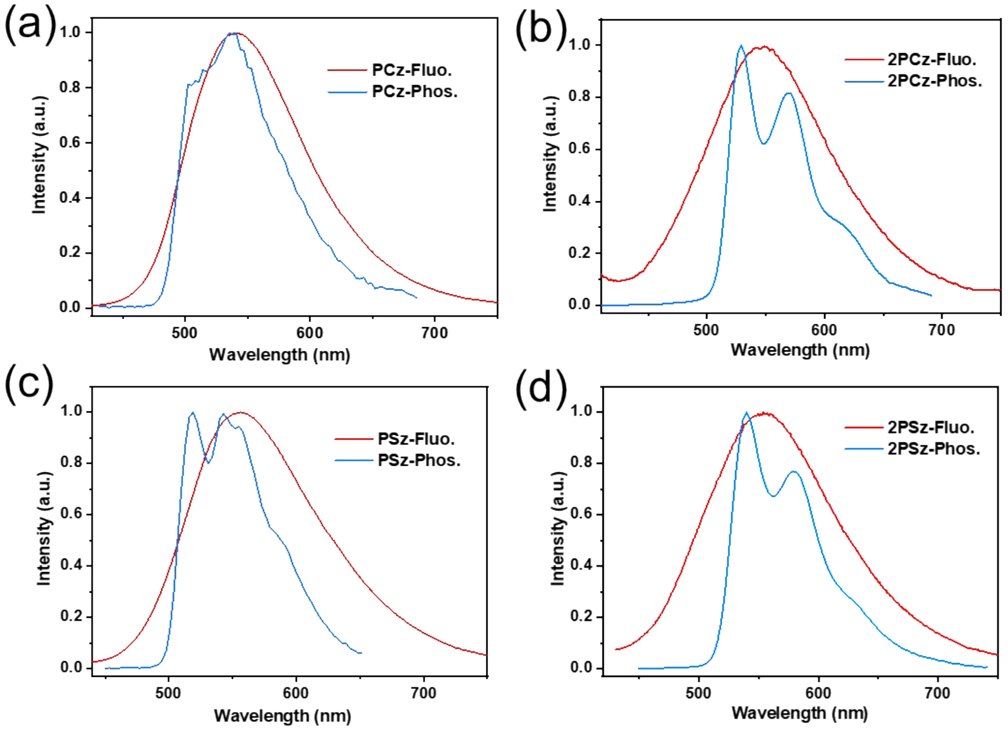

Figure S22. Fluorescence spectra at room temperature and phosphorescence spectra at 77 K for (a) **PCz**, (b) **2PCz**, (c) **PSz** and (d) **2PSz** films.

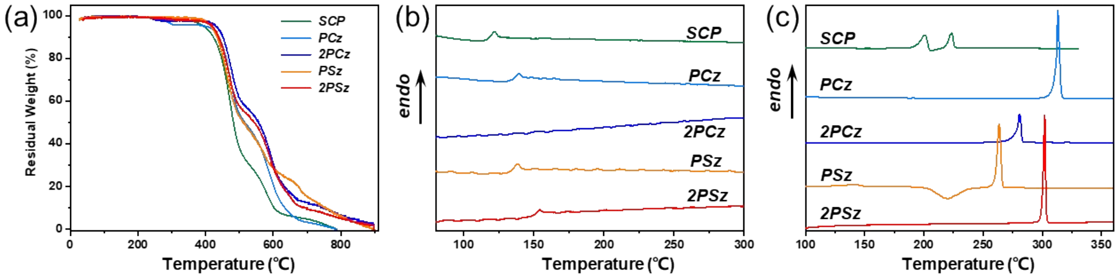

Figure S23. (a) Thermogravimetric analysis curves, (b) differential scanning calorimetry curves of measured under N_2, showing glass transition temperature (T_g), and (c) melting point temperature.

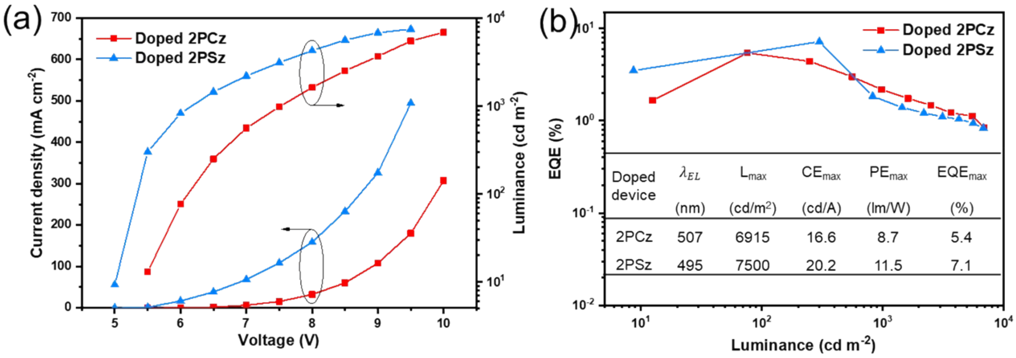

Doped device	λ_{EL} (nm)	L_{max} (cd/m^2)	CE_{max} (cd/A)	PE_{max} (lm/W)	EQE_{max} (%)
2PCz	507	6915	16.6	8.7	5.4
2PSz	495	7500	20.2	11.5	7.1

Figure S24. (a) Current density–voltage–luminance curves, and (b) EQE–luminance curves of **2PCz** and **2PSz** doped OLEDs, inset: a table summarizing EL performance.

References

1 Gaussian 09, Revision E.01, M. J. Frisch, G. W. Trucks, H. B. Schlegel, G. E. Scuseria, M. A. Robb, J. R. Cheeseman, G. Scalmani, V. Barone, G. A. Petersson, H. Nakatsuji, X. Li, M. Caricato, A. Marenich, J. Bloino, B. G. Janesko, R. Gomperts, B. Mennucci, H. P. Hratchian, J. V. Ortiz, A. F. Izmaylov, J. L. Sonnenberg, D. Williams-Young, F. Ding, F. Lipparini, F. Egidi, J. Goings, B. Peng, A. Petrone, T. Henderson, D.

Ranasinghe, V. G. Zakrzewski, J. Gao, N. Rega, G. Zheng, W. Liang, M. Hada, M. Ehara, K. Toyota, R. Fukuda, J. Hasegawa, M. Ishida, T. Nakajima, Y. Honda, O. Kitao, H. Nakai, T. Vreven, K. Throssell, J. A. Montgomery, Jr., J. E. Peralta, F. Ogliaro, M. Bearpark, J. J. Heyd, E. Brothers, K. N. Kudin, V. N. Staroverov, T. Keith, R. Kobayashi, J. Normand, K. Raghavachari, A. Rendell, J. C. Burant, S. S. Iyengar, J. Tomasi, M. Cossi, J. M. Millam, M. Klene, C. Adamo, R. Cammi, J. W. Ochterski, R. L. Martin, K. Morokuma, O. Farkas, J. B. Foresman and D. J. Fox, Gaussian, Inc., Wallingford CT, 2016.

2 C. Lee, W. Yang and R. G. Parr, Phys. Rev. B, 1988, **37**, 785−789.

3 T. Lu and F. Chen, *J. Comput. Chem*. 2012, **33**, 580−592.

4 S. D. Xu, T. T. Liu, Y. X. Mu, Y. F. Wang, Z. G. Chi, C. C. Lo, S. W. Liu, Y. Zhang, A. Lien and J. R. Xu. *Angew. Chem. Int. Ed.*, 2015, **54**, 874–878.

5 B. J. Xu, Y. X. Mu, Z. Mao, Z. L. Xie, H. Z. Wu, Y. Zhang, C. J. Jin, Z. G. Chi, S. W. Liu, J. R. Xu, Y. C. Wu, P. Y. Lu, A. Lien and M. R. Bryce, *Chem. Sci.*, 2016, **7**, 2201−2206.